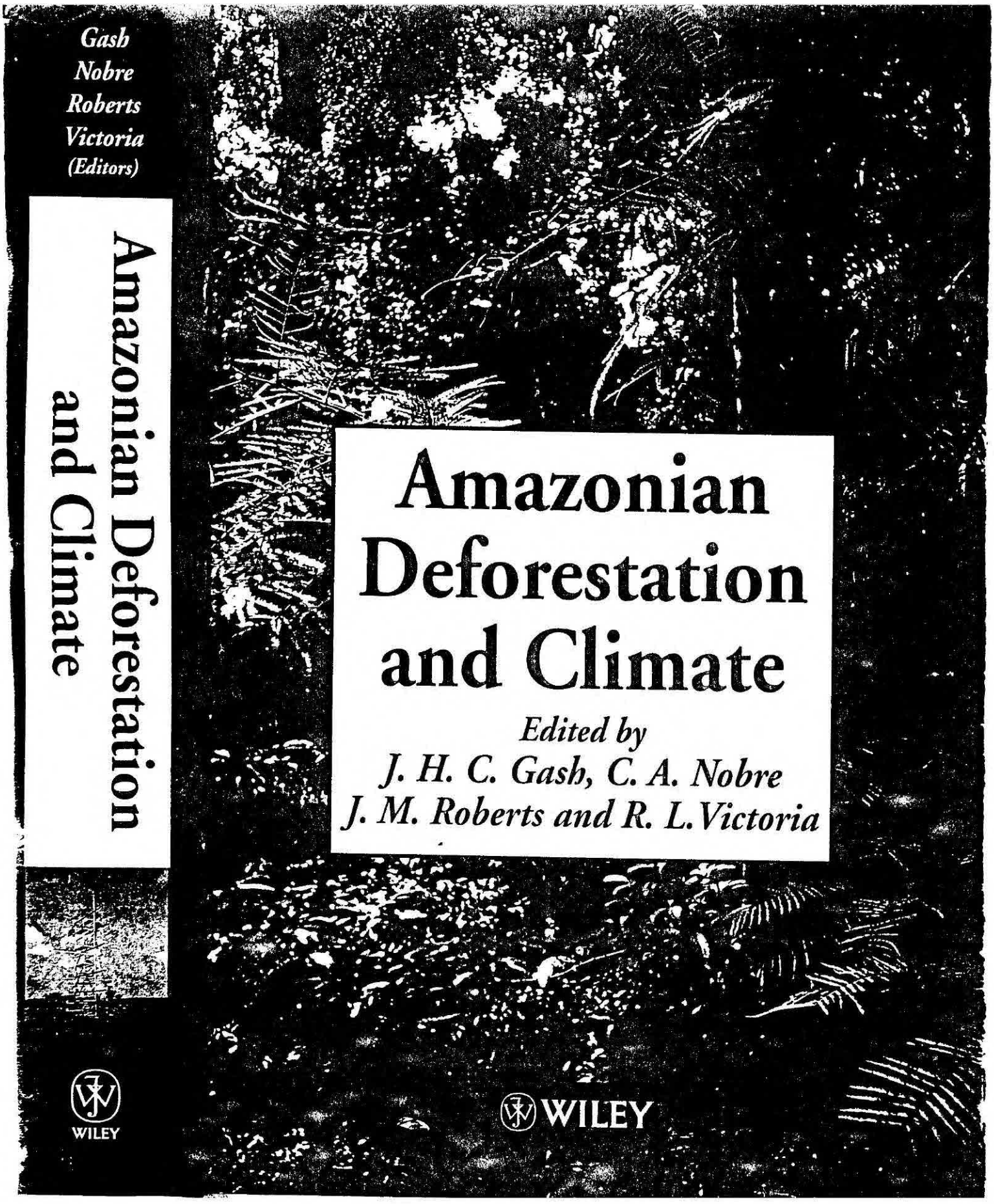
Gash
Nobre
Roberts
Victoria
(Editors)
Amazonian Deforestation and Climate
WILEY
Amazonian Deforestation and Climate
Edited by
J. H. C. Gash, C. A. Nobre
J. M. Roberts and R. L. Victoria
WILEY

Amazonian Deforestation and Climate

Edited by

J.H.C. GASH
Institute of Hydrology, UK
C.A. NOBRE
Centro de Provisão de Tempo e Estudos Climáticos, Brazil
J.M. ROBERTS
Institute of Hydrology, UK
R.L. VICTORIA
Centro de Energia Nuclear na Agricultura, Brazil

JOHN WILEY & SONS
Chichester • New York • Brisbane • Toronto • Singapore

29 A simulation of Amazonian deforestation using a GCM calibrated with ABRACOS and ARME data

A.O. MANZI[1] and S. PLANTON[2]
[1]*Instituto Nacional de Pesquisas Espaciais, São José dos Campos, Brazil*
[2]*Météo-France, Centre National de Recherches Météorologiques, Toulouse, France*

INTRODUCTION

The climatic effects of large scale deforestation are caused by complex interactions between the soil-vegetation system, clouds, radiation and the general circulation of the atmosphere. GCMs allow these to interact freely, making them uniquely powerful tools for simulating different climate change scenarios. A new land surface scheme ISBA (Intéractions Sol-Biosphère et Atmosphère) has been developed at CNRM (Centre National de Recherches Météorologiques), the research institute of Météo-France, for inclusion in the forecast, climate and mesoscale models. This scheme (Noilhan and Planton, 1989), despite its simplicity, represents all the principle physical processes present in more complex hydrological and ecological models of the soil-vegetation interface. Water and heat transfer through the soil depend on soil texture and moisture content; vegetation dependent processes such as the interception of rainfall and dew are treated explicitly, and transpiration is restricted by a surface resistance.

A first step in validating any soil-vegetation atmosphere transfer scheme consists of validating its ability to reproduce local scale observations of the water and energy balance. ISBA was tested and validated in this way using data from a variety of vegetation types and bare soil, drawn from the HAPEX-MOBILHY, FIFE and EFEDA datasets (Noilhan*et al.*, 1992). In this paper, these tests are enhanced by data from ARME (Amazon Region Micrometeorological Experiment, 1983 - 1985; Shuttleworth *et al.*, 1984a) and from ABRACOS (Gash *et al.*, 1996) to improve the ability of ISBA to represent tropical forest and the pasture which normally replaces it after deforestation. Further description of this work is given by Manzi (1993). The added realism gained by incorporating the ISBA scheme into EMERAUDE has allowed it to be used to simulate the impact of tropical deforestation.

The sensitivity of Amazonian climate to deforestation has been studied previously. Recent papers include those by Lean and Warrilow (1989), Nobre *et al.* (1991), Dickinson and Kennedy (1992), Dirmeyer (1992), Lean and Rowntree (1993), and

Amazonian deforestation and climate. Edited by J.H.C. Gash, C.A. Nobre, J.M. Roberts and R.L. Victoria.

Polcher and Laval (1994a and 1994b). The results of these modelling studies agree with regard to the sign of the resultant climatic changes but not always in their magnitude. The principal points on which they agree are the likely increase of the surface temperature and the reduction in evaporation and rainfall following deforestation. The motivation for carrying out another deforestation simulation is that the main climatic impacts are dependent on the individual models' representation of the physical processes, such as surface hydrology, convection and cloudiness, which are still poorly described and differ between models.

CALIBRATION OF ISBA WITH ARME AND ABRACOS DATA

A one-dimensional version of the ISBA surface scheme (Noilhan and Planton, 1989) was tested against observational data, both to verify the realism of the representation of the physical processes and to calibrate those parameters which could not be derived directly from the observations. In addition to the tests which were carried out using the data from HAPEX-MOBILHY, FIFE and EFEDA (Noilhan *et al.*, 1992) a one dimensional version of the model was tested against observational data from the ARME (Shuttleworth *et al.*, 1984a,b; Shuttleworth, 1988) and from ABRACOS (Gash *et al.*, 1996). These tests allowed verification of the ability of the model to reproduce the energy and water balances of equatorial rainforest and the tropical pasture which normally replaces it after deforestation.

AMAZONIAN FOREST

The ARME forest data were collected in the Reserva Ducke between September 1983 and September 1985, at the same site later used by ABRACOS (see Gash *et al.*, 1996). The site was considered representative of the *terra firme* forest (not seasonally flooded) of central Amazonia.

The tests carried out with the ARME data showed that some specific details of the parameterization needed to be improved. Firstly, because of the height of the vegetation it was necessary to introduce a zero plane displacement into the calculation of the turbulent exchange coefficients. Secondly it was necessary to introduce a term to account for the storage of heat in the vegetation, which can amount to up to 10 per cent of the daily net radiation. Adjusting the thermal coefficient of the vegetation, C_{veg}, to a value of $2\ 10^{-5}\ m^2KJ^{-1}$ gave correct simulation of heat storage in the forest soil-vegetation system, which agreed with the observations of Moore and Fisch (1986). This also improved the calculation of surface temperature, which was previously too low - particularly during the night. Without this calibration, *i.e.*, using the value of C_{veg} originally proposed by Noilhan and Planton (1989), ISBA calculates a flux from storage heat which is almost zero, producing night time surface temperatures which are too low.

Evaporation measurements after rainfall have shown that during the daytime water intercepted by forest canopies evaporates within a few hours. The ISBA scheme previously evaporated this water too rapidly and has therefore been modified to reduce the rate of evaporation of water intercepted by dense vegetation and giving a lower rate of evaporation for rainfall intercepted by the lower levels of the canopy.

Some parameters have been extracted directly from the data. Roughness length, z_0, has been taken as 2 m, and zero plane displacement, d, as 30 m. These values are consistent with those derived by other authors using the same dataset. Following the observations of McWilliam *et al.* (1993), for a similar site to Reserva Ducke, leaf area index, L^*, has been taken as 6.0. Taking into account the low values of radiation observed at the forest floor by Shuttleworth *et al.* (1984b) vegetation fraction, *veg*, has been taken as 0.99; for the albedo, α, the value of 0.12 reported in the same analysis has been used.

The calibration of the scheme was carried out on a selection of days on which the maximum amount of data were available. For these periods the thickness of the layer of hydrologically active soil (medium texture) was taken as 1 m.

Finally, a value of 250 sm^{-1} was derived for the minimum stomatal resistance per unit leaf area, R_{smin}, by fitting the model to the measured Bowen ratios.

The value of the maximum canopy interception capacity, $W_{rmax} = 0.1\ veg\ L^*$, was derived by running the scheme for a period of 25 months, forced by the observed atmospheric variables, and comparing the predicted interception loss with the measurements of Lloyd *et al.* (1988). Using the same approach a parameter sensitivity analysis was also carried out - the results can be summarised as:

(1) Reduction in z_0 modified the energy balance giving a reduction in evaporation (particularly evaporation directly from the soil and evaporation of intercepted water), and an increase in sensible heat flux and the amplitude of the daily surface temperature cycle.

(2) The effect of the initial value of the soil water reservoir on the energy balance is limited to the first month of the integration, the high rate of precipitation quickly produces an equilibrium situation with the soil moisture level close to saturation.

(3) Soil texture has very little effect on the energy or water balance.

(4) The effect of increasing the depth of the active soil layer on the energy balance is very small; however increasing the capacity of the soil water reservoir did cause an increase in runoff and reduced the seasonal variation in soil water content.

(5) The energy balance is highly sensitive to the vegetation fraction, *veg*. The relative contributions of evaporation directly from the soil and transpiration to the total evapotranspiration are strongly affected by the value of *veg*.

evapotranspiration are strongly affected by the value of *veg*.

AMAZONIAN PASTURE

Nineteen days of consecutive data from the first ABRACOS intensive observation period have been used. These were collected during the 1990 dry season (Wright *et al.*, 1992) at Fazenda Dimona (see Gash *et al.*, 1996) which is 80 km north of Manaus and about 80 km from the Reserva Ducke. Fazenda Dimona is an open clearing where, about 15 years previously, the forest had been replaced with cattle pasture by cutting and burning the primary forest, then sowing grass on the clay soil.

Most of the parameters needed to describe the ABRACOS site are available from the published results: a clayey soil covered with grass of leaf area index 1.2; a vegetation fraction of 0.85; a roughness length for momentum of 0.026 m; a zero plane displacement of 0.17 m; and an albedo of 0.163 (Wright *et al.*, 1992; Bastable *et al.*, 1993; and McWilliam *et al.*, 1993).

Using these parameter values in the calibration tests for the soil heat flux has allowed the mean thermal coefficient for the soil-vegetation system C_T to be evaluated as $3\ 10^{-5}$ m^2 kJ^{-1} and the mean thermal coefficient of the vegetation C_{veg} as $5\ 10^{-5}$ m^2 kJ^{-1}. This adjustment to the previously assigned values gave much improved prediction of the surface temperature, which was otherwise too low during the night. ISBA has been calibrated against the ABRACOS data in three stages. In the first stage the roughness length for vapour and sensible heat transfer has been taken as being the same as that for momentum transfer. This is the assumption made in most surface schemes and which was made in the version of ISBA incorporated into the EMERAUDE GCM (Manzi and Planton, 1994).

An optimised value of the minimum surface resistance of 144 s m^{-1} gave very satisfactory agreement between the observed energy balance and that calculated by ISBA - both for the daily trend and for the cumulative values of the fluxes.

The cumulative evapotranspiration predicted by ISBA for the whole period was 47 mm, which can be compared with the observed value of 46 mm. Evaporation directly from the soil, transpiration, and evaporation of intercepted water amounted to 33, 64 and 3 per cent respectively of the total evapotranspiration, however this result cannot be validated as separate measurements of the components were not made. The loss of water as evapotranspiration and the gains by rainfall and dew are balanced by the observed variation in soil moisture content down to a depth of approximately 2 m.

The second stage of the calibration took account of the differences in roughness length between vapour and sensible heat transport, and that for momentum. These tests allow comparison between the surface temperature, T_s, predicted by ISBA with those estimated by Wright *et al.* (1992) who took $ln(z_{0m}/z_{0h}) = 2$, as suggested by Brutsaert (1982). Good agreement between T_s as calculated by ISBA and as by Wright *et al.* is obtained with $ln(z_{0m}/z_{0h}) = 2.3$. The amplitude of the cycle of T_s is increased by 2.5 °C compared to the case when $ln(z_{0m}/z_{0h}) = 2$. This increase is dominated by the maximum temperature being raised by 2 °C, which causes an

calibrated to reproduce the surface resistance estimated from the Penman-Monteith model. With the assumption that the vegetation totally covers the ground ($veg = 1$) and $z_{0m} = 10\ z_{0h}$, ISBA correctly reproduced the observed surface resistance and energy balance. However, the observed vegetation cover is not unity and sensitivity studies have shown that ISBA is very sensitive to vegetation cover, particularly the estimates of direct evaporation from the soil. (Jacquemin and Noilhan, 1990; Manzi, 1993). Therefore, when there is incomplete surface cover the surface resistance calculated by ISBA is not comparable to that calculated by the Penman-Monteith equation.

It can be concluded that ISBA allows several combinations of parameters for tropical pasture, all of which are capable of satisfactorily reproducing the observed reduction in evaporation in a drying soil. The only real improvement to the predictions that can be obtained by taking into account the difference between z_{0m} and z_{0h}, appears to be the slightly higher surface temperature of approximately 2 °C. This, together with the fact that after the calibration, tests with $z_{0m} = z_{0h}$ gave results that were just as good those with z_{0m} z_{0h} justifies not complicating ISBA, either by introducing procedures to account for the differences in transport of vapour and sensible heat compared to momentum, or by introducing different coefficients to describe the controls on surface resistance.

THE EMERAUDE MODEL

The GCM EMERAUDE is the spectral model used by Météo-France for short range operational forecasting between 1985 and 1991 (Ernie, 1985; Coiffier *et al.*, 1987; Geleyn *et al.*, 1988). The version used for the experiments reported here includes the modifications by Royer *et al.* (1990) and Planton *et al.* (1991) to improve the model's ability to make climate simulations. The horizontal resolution corresponds to a T42 truncation, so that the physical processes are resolved on a Gaussian grid of approximately 2.8° by 2.8°. There are 20 levels in the vertical, with five levels in the troposphere below 2000 m. The physical parameters include: radiation with interactive cloudiness, deep convection with a Kuo-type scheme, large scale precipitation, and orographic gravity waves. Boundary layer processes and turbulence are represented by the parameterization scheme of Louis *et al.* (1981).

METHOD

Two model runs each of 50.5 months were carried out with EMERAUDE coupled to the ISBA surface scheme: a control run where the vegetation has been classified according to Wilson and Henderson-Sellers (1985), and a deforested run in which the original humid tropical forest was replaced by grassland. The control run is identical to that described as the "ISBA experiment" by Manzi and Planton (1994), except that the integration time has been increased by 12 months. The only difference between

the control run and the deforested run is the change made to the Amazonian vegetation.

The model runs were initialised using climatological snow and ice cover. Sea surface temperature was specified throughout the experiment using AMIP monthly data fields given by COLA/CAC (Center for Ocean-Land-Atmosphere Studies and NOAA Climate Analysis Center) averaged over the ten year period 1979-1988 (Gates, 1992). The initial state of the atmosphere was that on 15 December 1983, interpolated from the ECMWF (European Centre for Medium-Range Weather Forecasting) analysis. The initial soil moisture content was the climatological value given by Mintz and Serafini (1989) using the formula

$$w_s = w_2 = H_{ser}(w_{fc} - \text{veg}\, w_{fl} - 0.02) + \text{veg}\, w_{fl} + 0.02 \quad (1)$$

where w_s and w_2 are the volumetric water content of the surface and lower reservoirs respectively; H_{ser} is the Mintz and Serafini (1989) climatological relative humidity, which varies between 0 and 1; w_{fc} and w_f are volumetric soil water content at field capacity and the wilting point respectively; and 0.02 is the minimum value of soil water content obtained by Manzi and Planton (1992) during a previous annual integration of EMERAUDE with ISBA. This equation gives the maximum value equivalent to field capacity when H_{ser} is equal to unity, and when H_{ser} is zero gives values slightly above wilting point for vegetation with complete canopy cover and very low values for bare soil. For both simulations the deep soil temperature is reset to a climatological value derived from the ECMWF analysis every twenty days. The soil water content is not reset.

Table 1 shows the values of the parameters used in ISBA to describe tropical forest and pasture. For the forest case these parameters have been calibrated with the ARME data as described in Section 2. For the pasture case the parameters were prescribed in a similar way to other recent deforestation experiments (for example Nobre *et al.*, 1991). The characteristics of this hypothetical grassland are similar to the parameters calibrated against the ABRACOS data collected over actual Amazonian pasture, as described in Section 2. The actual values derived in Section 2 could not be used as the data were not available until after the model experiments were completed.

The extent of the modelled deforestation can be seen in Figure 1 from the difference between the roughness lengths of the original forest and the modelled pasture, which

Table 1 The ISBA parameters representing Amazonian forest and the grassland which replaces it in the deforestation experiment

	albedo	leaf area index (L*)	R_{smin}/L (sm^{-1})	z_0 (m)	d (m)	veg.	depth of soil (m)
forest	0.13	6	42	2	28	0.99	4
grass	0.20	2	75	.06	.20	0.85	2

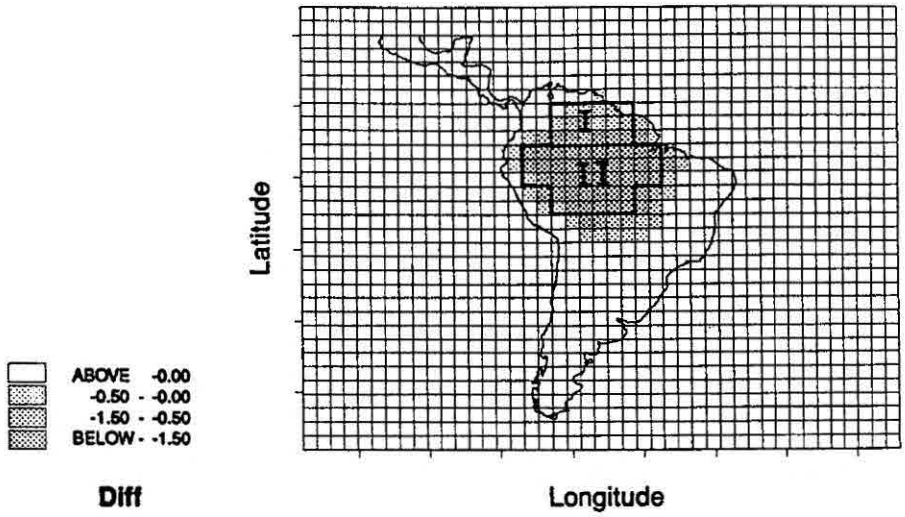

Figure 1 The extent of deforestation represented by the surface roughness length anomaly (grass minus forest). The areas chosen to represent northern and southern Amazonia are shown as I and II respectively.

is reduced from 2.0 m for the forest to 0.06 m for the pasture. This reduction in aerodynamic roughness modifies the wind field in the lower layers of the model and interacts strongly with the dynamics of the model.

The albedo for diffuse solar radiation is increased with deforestation from 13 to 20 per cent, which causes a decrease in surface net radiation and a reduction in convection and humidity convergence. The other important difference between the two vegetation types is the decrease, from 4 to 2 m, in the depth of the hydrologically active soil layer. This reduction in soil water holding capacity can create increased runoff and also reduction in evapotranspiration during the driest periods.

The increase in minimum surface resistance ($R_{sm} = R_{smin}/L^*$) for the grass, compared to the forest, reduces the transpiration, whilst the reduction in leaf area index, coupled with the reduction in roughness length, reduces the interception loss. On the other hand the increase in the fraction of bare soil (1 - veg) can contribute to increasing evaporation directly from the soil, which in part compensates for the reduction in transpiration and interception.

RESULTS AND DISCUSSION

The results have been averaged over three years of integration (from the 2 March to 5 February). The first 14.5 months, from initialisation on 15 December to the end of February 14.5 months later, have been ignored. This allows the model to reach a stage of quasi-equilibrium, with only a weak dependence on the initial soil water content.

Figure 2 shows the anomalies (deforestation minus control) for the fields of

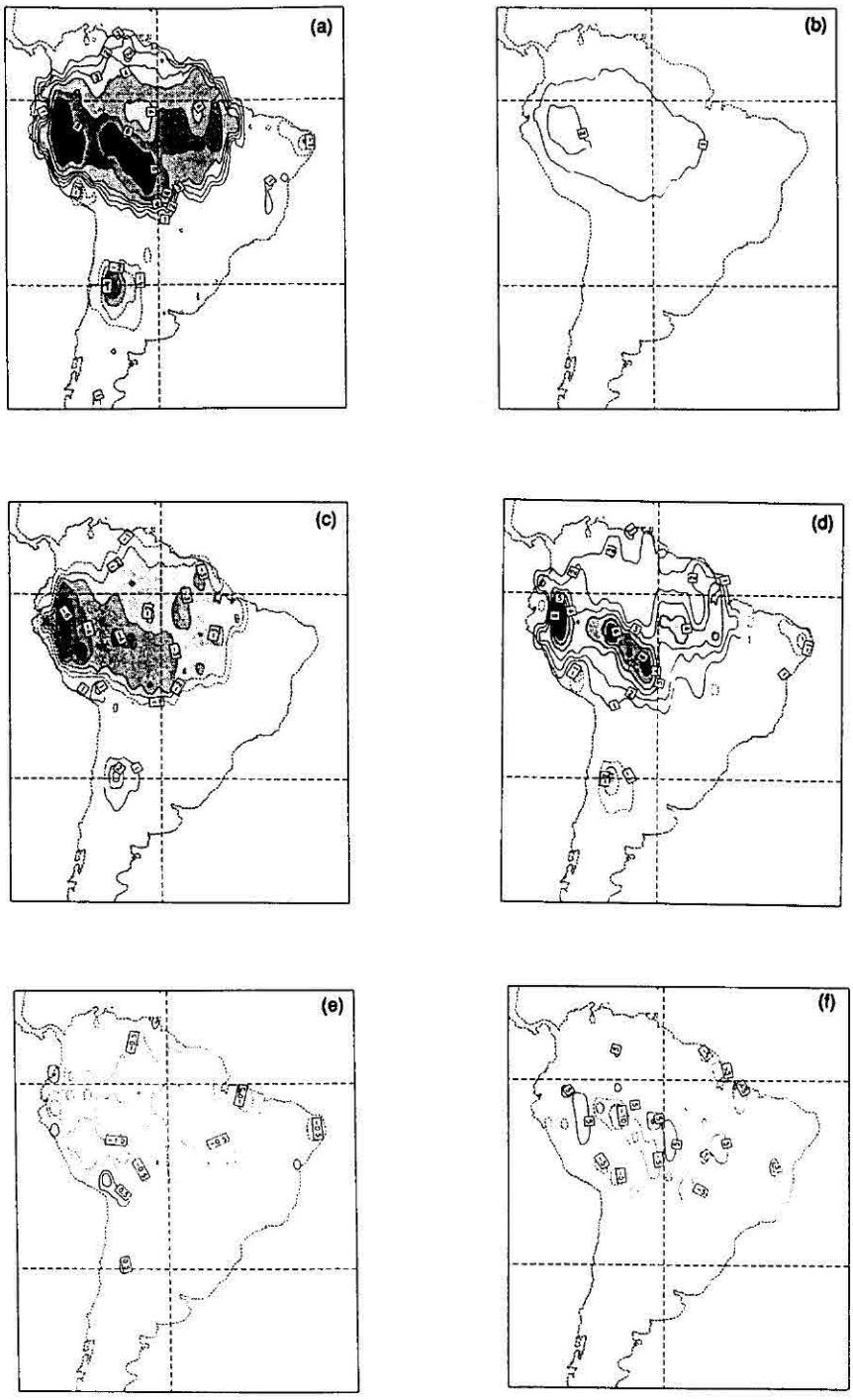
(a)
(b)
(c)
(d)
(e)
(f)

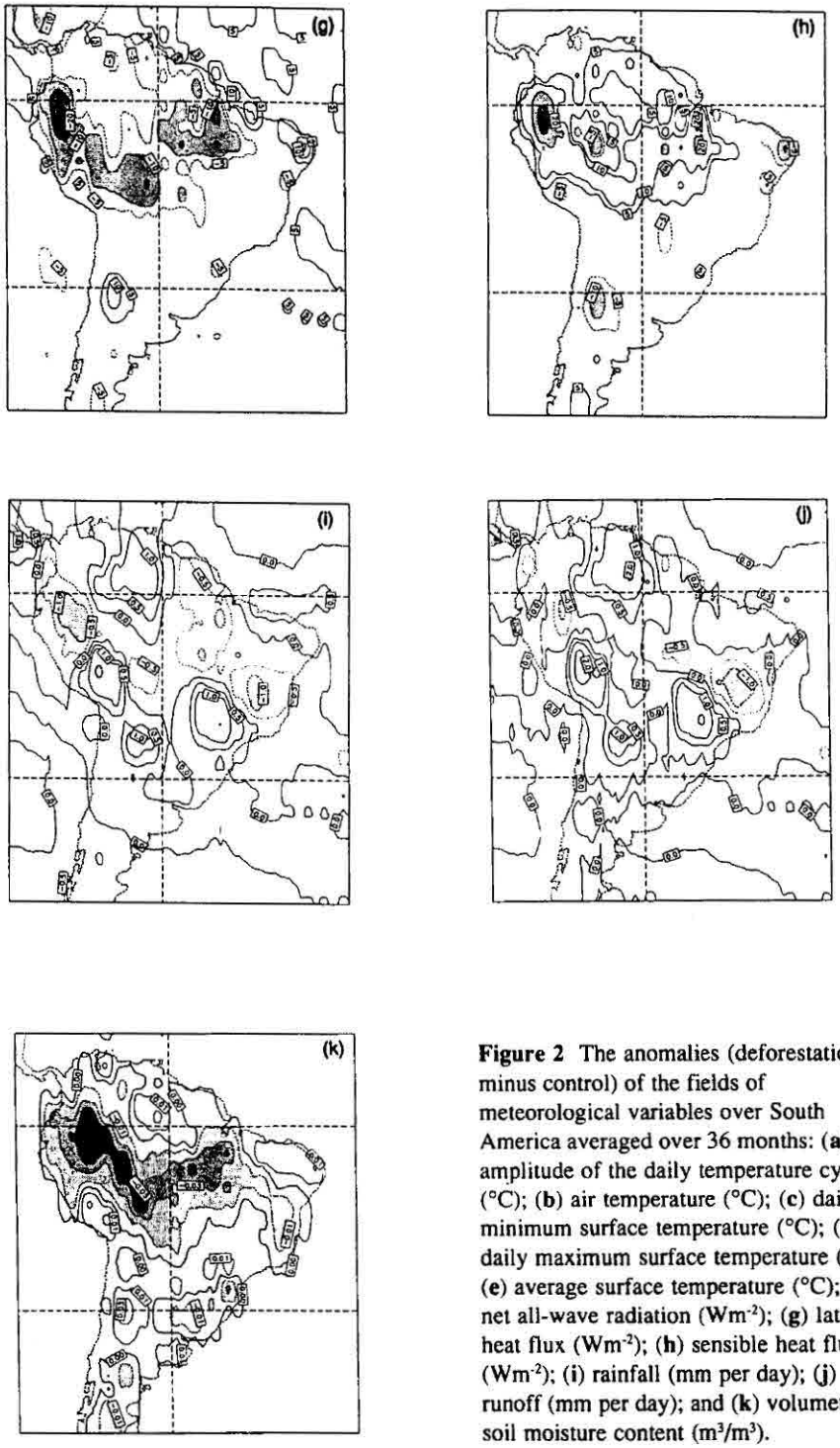

Figure 2 The anomalies (deforestation minus control) of the fields of meteorological variables over South America averaged over 36 months: (**a**) amplitude of the daily temperature cycle (°C); (**b**) air temperature (°C); (**c**) daily minimum surface temperature (°C); (**d**) daily maximum surface temperature (°C) (**e**) average surface temperature (°C); (**f**) net all-wave radiation (Wm^{-2}); (**g**) latent heat flux (Wm^{-2}); (**h**) sensible heat flux (Wm^{-2}); (**i**) rainfall (mm per day); (**j**) runoff (mm per day); and (**k**) volumetric soil moisture content (m^3/m^3).

meteorological variables averaged over the 36 months discussed above. The analysis has been limited to the region which has been deforested. The control run has been analysed by Manzi and Planton (1994) for the first 38.5 months and no significant changes have been detected in the extra 12 months. The values of these variables, averaged over the 36 months, are also presented in the pairs of Tables 4 and 5, 6 and 7, and 2 and 3 respectively for Region I (north), Region II (south) and Region I + II (total) as defined in Figure 1. Monthly values averaged over Region I + II, and over the last three years of the integration (both deforested and control) are given in Figure 3. In the north of Amazonia (shown as Region I in the figure) the wet season occurs during the northern hemisphere summer, whereas the wet season further south (Region II) occurs in the first months of the year (Figueroa and Nobre, 1990).

Figures 3c and 3j show the average monthly radiation and rainfall respectively measured at the Reserva Ducke site, near Manaus, during the 25 months of the ARME (Shuttleworth, 1988; Lloyd *et al.*, 1988; Manzi, 1993). The estimates of evapotranspiration and interception produced by ISBA (Noilhan*et al.*, 1992; Manzi, 1993) are shown in Figures 3h and 3i, respectively. The ARME results are presented as a separate line since they represent the particularly humid conditions of Manaus, whereas the modelling experiments are averaged over the whole of Amazonia, with its varied climatic conditions. However, the model predictions are in good general agreement with the observations, with the exception of the dry season, which is predicted to be too short and two months early in comparison with the observations. The model also predicts a second less-rainy period which does not occur in Manaus.

Following the modelled deforestation, the amplitude of the daily surface temperature cycle (Figure 2a) increased by an average of 6 °C. This increase in amplitude is the result of an increase of 3 °C in the daily maximum temperature (Figures 2d and 3e) and a decrease of 3 °C in the daily minimum. The average surface temperature is slightly decreased by about 0.5 °C (Figures 2e and 3d, and Table 2), but the temperature of the air close to the surface increased by an average of 1.3 °C (Figure 2b and Table 2). The increase in average air temperature, but decrease in the average surface temperature, is explained by the fact that the turbulent transfer is more efficient during the day when the surface temperature is higher over the grass than the forest.

The increase in the amplitude of the daily temperature cycle has also been found in other deforestation simulations (for example: Lean and Warrilow, 1989; Nobre*et al.*, 1991; Dickinson and Kennedy, 1992). They report an increase in maximum surface temperature, which produces an increase in average surface and air temperature. In the simulation reported by Polcher and Laval (1994b) the average surface temperature and the amplitude of the daily cycle are both slightly decreased by deforestation. The ABRACOS observations reported by Bastable *et al.* (1993) showed that the amplitude of the daily temperature cycle was greater over grass than over nearby forest, principally during the dry season, but that the average temperature was the same for the two vegetation types. In agreement with our results this was found for both dry and wet seasons.

The impact of deforestation on the temperature field is more important in Region

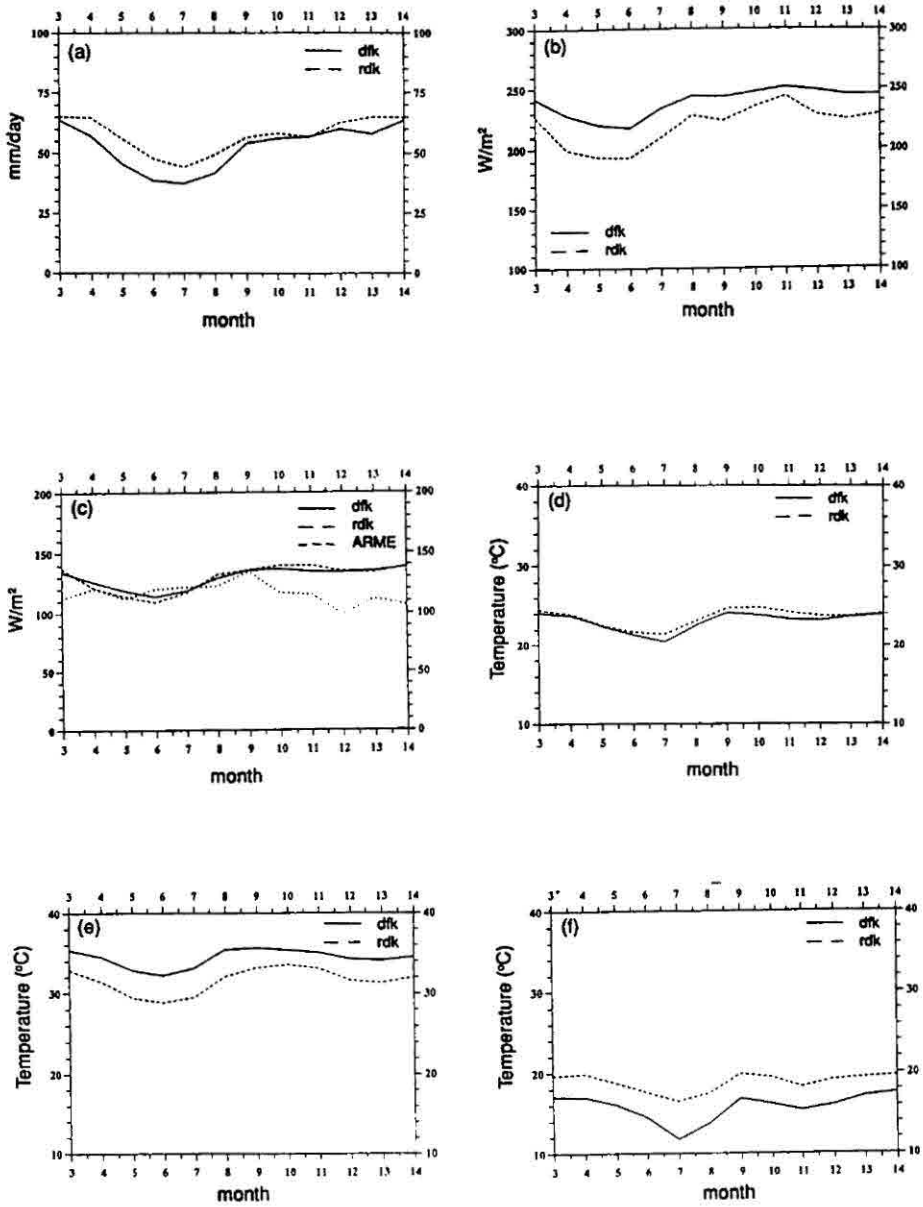

Figure 3 Monthly averages, over the 36 months for the whole of Amazonia (Regions I and II) for the deforestation experiment (solid line) and the control run (dashed line) and the ARME observations (dotted line): (**a**) cloudiness (%); (**b**) incident solar radiation (Wm^{-2}); (**c**) net all-wave radiation (Wm^{-2}); (**d**) average surface temperature (°C); (**e**) daily maximum surface temperature (°C); (**f**) daily minimum surface temperature (°C).

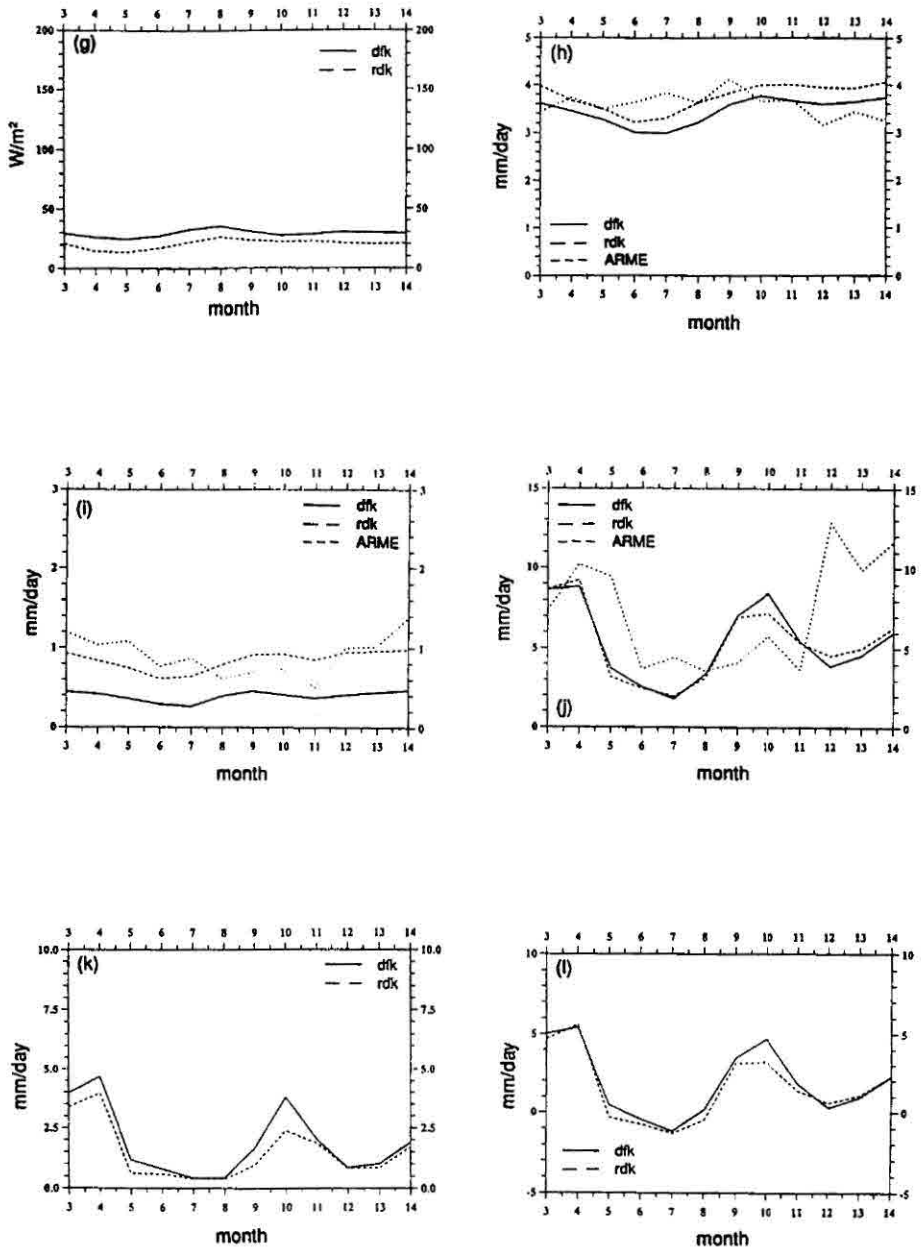

Figure 3 (contd.) (**g**) sensible heat flux (Wm^{-2}); (**h**) evapotranspiration (mm per day); (**i**) interception (mm per day); (**j**) rainfall (mm per day) (**k**) runoff (mm per day); and **l**) rainfall minus runoff (mm per day).

Table 2 The energy balance of Amazonia (Regions I and II) over the 36 months of the deforestation and control runs. S_D is the incident solar radiation; $(1 - \alpha)S_D$ is the net solar radiation; L_D is the downward longwave radiation; L_n is the net longwave radiation; R_n is the net all-wave radiation; LE is latent heat flux; H is sensible heat flux T_s(mean), T_s(max) and T_s(min) are the mean, daily maximum and daily minimum surface temperatures; T_a is air temperature at the lowest model level; N(tot) and N(low) are the percentages of total and low cloud cover; and U_a is horizontal windspeed at the lowest model level. Fluxes are expressed in Wm^{-2}, temperatures in °C and windspeed in ms^{-1}.

	S_D	$(1-\alpha)S_D$	L_D	L_n	R_n	LE	H	T_s (mean)	T_s (max)	T_s (min)	T_a	N (tot)	N (low)	U_a
control	218	191	376	62	129	109	19	23.5	31.4	18.8	24.4	58	38	2.2
deforested	238	196	370	66	130	100	29	23.0	34.3	15.8	25.7	53	30	4.0
deforested – control	20	5	-6	4	1	-9	10	-0.5	2.9	-3.0	1.3	-5	-8	1.8

II (Table 3), to the south of the Equator, than in Region I (Table 4) to the north. This result is also found for the meteorological variables. On average there is no change to the net radiation, R_n (Figures 2f and 3c). Figure 3a shows that total cloudiness is reduced by about 5 per cent for the deforested region, but this is not uniform in the vertical. There was in fact a decrease of more than 8 per cent in low cloud amount, but this was partly compensated for by an increase in high cloud. The reduction in

Table 3 The energy balance of Region II of Amazonia for the 36 months of the deforestation and control run

	S_D	$(1-\alpha)S_D$	L_D	L_n	R_n	LE	H	T_s (mean)	T_s (max)	T_s (min)	T_a	N (tot)	N (low)	U_a
control	221	193	374	65	128	106	23	23.7	32.1	18.6	24.7	56	35	2.1
deforested	244	199	367	71	128	95	35	23.2	35.7	15.1	26.2	50	26	4.3
deforested – control	23	6	-7	6	0	-11	12	-0.5	3.6	-3.5	1.5	-6	-9	2.2

Table 4 The energy balance of Region I of Amazonia for the 36 months of the deforestation and control run.

	S_D	$(1-\alpha)S_D$	L_D	L_n	R_n	LE	H	T_s (mean)	T_s (max)	T_s (min)	T_a	N (tot)	N (low)	U_a
control	212	185	380	55	130	117	9	23.0	29.9	19.1	23.7	62	46	2.4
deforested	226	188	376	56	131	113	15	22.5	31.1	17.1	24.5	59	40	3.3
deforested – control	14	3	-4	1	1	-4	6	-0.5	1.2	-2.0	0.8	-3	-6	0.9

result is also found for the meteorological variables. On average there is no change to the net radiation, R_n (Figures 2f and 3c). Figure 3a shows that total cloudiness is reduced by about 5 per cent for the deforested region, but this is not uniform in the vertical. There was in fact a decrease of more than 8 per cent in low cloud amount, but this was partly compensated for by an increase in high cloud. The reduction in cloud cover leads to an average 20 Wm^{-2} increase in solar radiation reaching the surface. Because the albedo of the grass is higher than that of the forest some of this excess radiation is reflected by the surface and the net solar radiation over the grass is increased by only 5 Wm^{-2} compared to the forest. The downward longwave radiation is also reduced by about 6 Wm^{-2} as a result of the decreased cloud cover. However, the average surface temperature of the grass is less than the forest and it emits an average of about 2 Wm^{-2} less than the forest. The net longwave loss is thus increased by an average of about 4.5 Wm^{-2} and the net all-wave radiation increased by less than 1 Wm^{-2} (1.4 Wm^{-2} north of the Equator and 0.2 Wm^{-2} to the south). This increase is in contrast to other simulations of Amazonian deforestation. For example Lean and Warrilow (1989) reported a decrease in R_n of 21 Wm^{-2} as a result of the increase in surface albedo. In this case the longwave radiation did contribute, since with an increase in albedo of 5.2 per cent, in their simulation, it would have been necessary for the average incident solar radiation to have been above 400 Wm^{-2} to reduceR_n by 21 Wm^{-2} (whereas it did not exceed 250 Wm^{-2}). Nobre*et al.* (1991) used a fixed climatological cloudiness and found a reduction of 26 Wm^{-2} in R_n, which resulted in an increase of 8 Wm^{-2} in longwave loss (caused by an increase in surface temperature) and a decrease of 18 Wm^{-2} in net solar radiation (caused by an increase in the albedo). Dickinson and Kennedy (1992) also reported a decrease of 18 Wm^{-2} in R_n, dominated by an increase in longwave loss of 15 Wm^{-2}. This result was attributed to a reduction in the incident longwave radiation, caused by 7 per cent less cloud cover - the increase in incident solar radiation was compensated by the higher albedo of the grass. The disagreement between these simulations shows the strong dependence of the results of model experiments on the parameterization of clouds and radiative transfer. In fact, for Lean and Warrilow (1989) and Nobre*et al.* (1991) the decrease in net radiation at the surface is dominated by the effects of albedo, whilst for Dickinson and Kennedy (1992) it is dominated by changes to the longwave balance. In the simulation described in this paper the increase in longwave loss is compensated by an increase in net incident solar radiation.

Following deforestation the average latent heat flux (LE) decreased by 9 Wm^{-2} and the average sensible heat flux (H) increased by the same amount. The Bowen ratio, H/LE, therefore increased from 0.17 over the forest to 0.26 over the grass (Table 2). These changes do not occur uniformly over the whole area of deforestation - they are greater to the south of the Equator (Table 6) than to the north (Table 4). However, monthly mean evapotranspiration for the grass averaged over the whole region is always less than that for the forest (Figure 3h) and the sensible heat flux is always greater (Figure 3g). This comparatively lower latent heat flux from the grass is caused by a strong reduction in transpiration and the evaporation of intercepted water, which is only partly compensated by increased evaporation directly from the soil (Table 5,

Table 5 The water balance of Amazonia (Regions I and II) over the 36 months of the deforestation and control runs. P is rainfall; E evapotranspiration; R runoff; E_{tr} transpiration; E_g evaporation from the soil; I is interception (all expressed in mm per day). Ptt is precipitable water (mm) and HU_{soil} is relative soil moisture (%).

	P	E	R	E_{tr}	E_g	I	Ptt	HU_{soil}
control	5.33	3.78	1.51	2.44	0.51	0.83	37.43	82.3
deforested	5.29	3.47	1.84	1.74	1.33	0.39	37.04	76.2
deforested – control	-0.4	-0.31	0.33	-0.69	0.82	-0.44	-0.38	-0.61

Table 6 The water balance of Region I of Amazonia for the 36 months of the deforestation and control run

	P	E	R	E_{tr}	E_g	I	Ptt	HU_{soil}
control	6.47	4.04	2.43	2.45	0.97	0.62	37.33	100.0
deforested	6.97	3.90	3.15	2.02	1.49	0.39	37.81	100.0
deforested – control	0.50	-0.14	0.72	-0.43	0.52	-0.23	0.48	0.0

Table 7 The water balance of Region I of Amazonia for the 36 months of the deforestation and control run

	P	E	R	E_{tr}	E_g	I	Ptt	HU_{soil}
control	4.83	3.67	1.12	2.43	0.31	0.92	37.47	74.7
deforested	4.56	3.28	1.27	1.63	1.26	0.40	36.72	65.9
deforested – control	-0.27	-0.39	01.6	-0.81	0.95	-0.53	-0.75	-8.8

6 and 7). The reduction in transpiration is due to the reduced canopy cover and increased minimum surface resistance. The reduction in evaporation of intercepted water is caused both by the smaller canopy capacity of the grass, 0.3 mm, compared to the forest, 0.6 mm, and by the reduction in roughness length from 2 m for the forest to 0.06 m for the grass. The increase in direct evaporation from the soil follows from the increased proportion of exposed soil in the grassland and the high rainfall climate.

The reduction in evapotranspiration of about 8 per cent (0.31 mm per day) is less than that found in the other experiments discussed previously: 27 per cent (0.85 mm per day) by Lean and Warrilow, 30 per cent (1.36 mm per day) by Nobre *et al.*, and 20 per cent (0.7 mm per day) by Dickinson and Kennedy (1992). However the reduction is in good agreement with that found by Polcher and Laval (1994b), 11 per cent (0.35 mm per day). The different response of these various models is mainly associated with the performance of their surface schemes, but also with the model calculations of available energy and rainfall. For Lean and Warrilow (1989) the

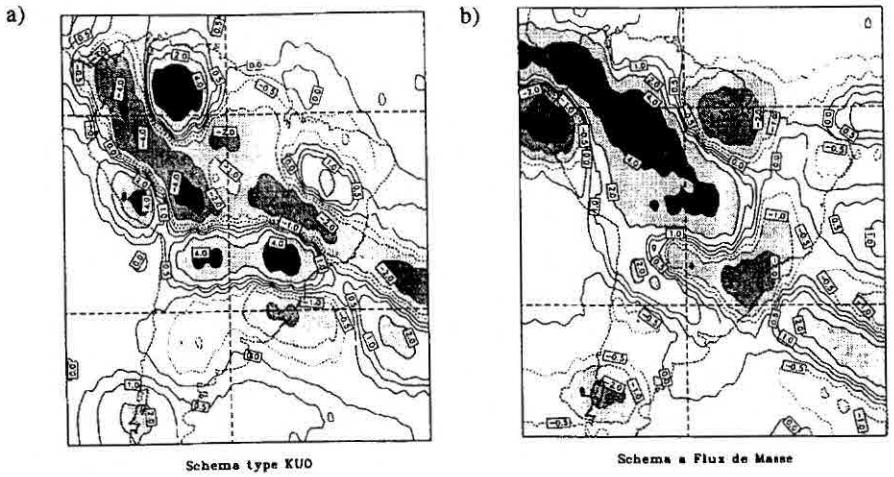

Figure 4 Anomalies in the rainfall fields (mm per day) for the deforestation minus control run for a) the Kuo-type convection scheme and b) the mass flux convection scheme averaged over January to March inclusive. The dotted lines represent negative values.

reduction in evapotranspiration (which was dominated by the interception loss) was attributed to the reduction in roughness and is the same size as the reduction in R_n. Dickinson and Kennedy (1992) reported a similar conclusion from their experiment. However Nobre *et al.* (1991) found that transpiration and evaporation directly from the soil accounted for 70 per cent of the reduction in evapotranspiration. In the deforestation simulation reported here the reduction in evapotranspiration is mainly caused by reduced evaporation of intercepted water, as shown in Figure 3i, since the reduction in transpiration is compensated by the increased evaporation from the soil surface.

It is important to note that the deforested areas chosen by the various authors are not necessarily coincident. However, with the exception of Polcher and Laval (1994b), they all represent the greater part of Amazonia. Polcher and Laval averaged over an area which was smaller than the area used here.

Rainfall is reduced in some places, but is increased in others (Figure 2i). It increases particularly in the north, south-west and south-east of Amazonia. This clearly implies that the deforestation produces a change in atmospheric circulation over Amazonia. The mean monthly rainfall over Amazonia is shown in Figure 3j, which shows that there is no stable tendency in the monthly regional rainfall anomaly during the year after deforestation. This seems to result from the seasonal cycle of moisture convergence (taken as the difference between rainfall and evapotranspiration) (Figure 3l). However the runoff is always higher from the grass compared to the forest (Figure 3k). The anomalies in the runoff field (Figure 2j) follow those in the rainfall field (Figure 2i).

Figures 3 and 5 show that the water balance is intensified to the north of the Equator

with the exception of a slight decrease in the evapotranspiration) with an increase n rainfall. This increase is likely to be caused by the combination of higher wind-speeds close to the ground surface and the more pronounced topography in that region. The hydrological cycle is certainly less intense south of the Equator, with a reduction in rainfall of 0.27 mm per day (5.5 per cent) and of evapotranspiration of 0.39 mm per day (10.5 per cent) for the grassland compared to the control run. Nevertheless the runoff and the moisture convergence has been slightly increased. The relative moisture content of the soil (HU_{soil} in Tables 5, 6 and 7, defined here as the difference between actual soil moisture content and that at the wilting point, normalised by the difference between soil moisture content at field capacity and at the wilting point) is less for the grassland to the south of the Equator, but is not changed to the north – where soil moisture content never falls below field capacity for either vegetation type.

The response to the deforestation can be most clearly seen in its effect on soil moisture content. This is shown in Figure 2k, where it can be seen that those areas with reduced soil moisture content correspond exactly to those areas where the rainfall has been reduced (Figure 2i), which are also the areas with the strongest reduction in evapotranspiration (Figure 2i), greatest increase in maximum surface temperature (Figure 2e), and greatest increase in sensible heat flux (Figure 2h).

It is difficult to conclude whether or not the modification to the rainfall field in the grassland is a direct result of the reduction in evapotranspiration. As is shown in the next section, it appears that the reduction in evapotranspiration, and thus the change in the atmospheric circulation over the deforested region is brought about by the effect of surface roughness. It can also be seen from Tables 2, 4 and 6 that there is a strong increase, of a factor two, in the surface windspeed.

Contrary to the results of the other deforestation experiments discussed here Tables 5, 6, and 7 show that the moisture convergence has increased over the region after deforestation, partly compensating for the reduction in evapotranspiration. It can also be seen from these tables that the precipitable water vapour content (the specific humidity integrated over a complete vertical column of the atmosphere) has not changed significantly.

SENSITIVITY TO THE ALBEDO AND SURFACE ROUGHNESS

As has been shown in numerous numerical climate simulations (see the review by Rowntree, 1991) anomalies in albedo and surface roughness can produce significant changes in the atmospheric circulation. Deforestation modifies both of these parameters, and therefore, to separate the effects of these changes two additional short simulations were carried out, each of three months duration and covering the period December to February inclusive. The initial conditions for these two simulations are taken from the predictions of the control run at the end of November on the first year of integration – i.e. 11.5 months after the start of the integration. In the first experiment all the parameters in ISBA representing the forest have been retained, apart from the

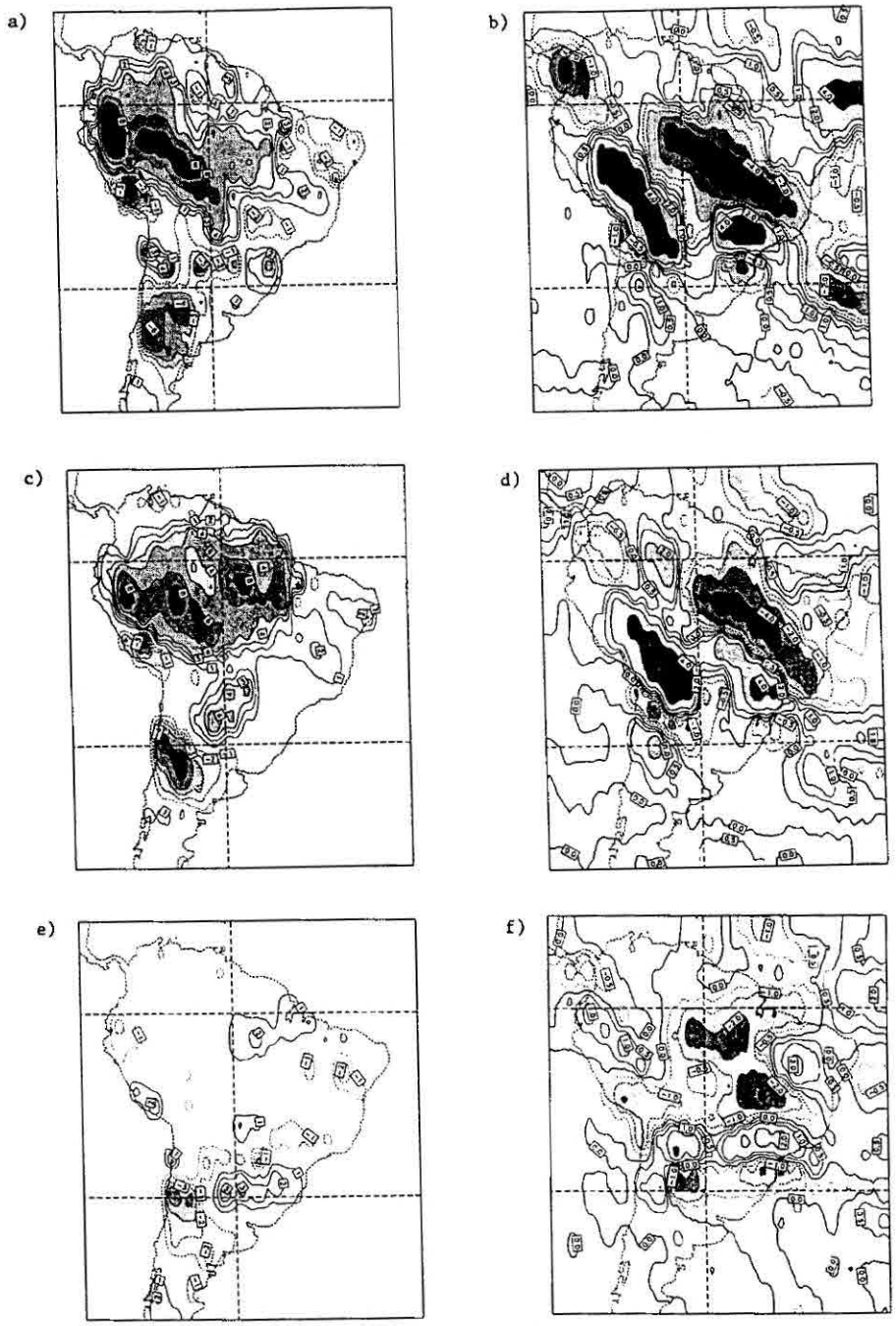

Figure 5 Anomalies in the fields of the amplitude of the daily surface temperature cycle (°C) and rainfall (mm per day) for the following experiments respectively: (a) and (b) complete deforestation minus control; (c) and (d) change in roughness length minus control; (e) and (f) change in albedo minus control.

roughness length which has been changed to the post-deforestation value. In the second experiment all the forest parameters were retained and the albedo was changed. These two simulations were then compared with control and deforested model runs for the same three month period.

The energy balance parameters and hydrological averages for Region II (see Figure 1) are given in Table 8. The analysis has been limited to Region II because it is entirely covered in tropical forest during the control run, and the impact of deforestation is currently stronger in that part of Amazonia. The map showing the anomalies in the fields of the amplitude of the daily surface temperature cycle and rainfall over South America are shown in Figure 5, for the three cases: deforestation minus control, roughness change minus control and albedo change minus control.

The albedo increase changes the radiation balance by reducing the net solar radiation and thus the net all-wave radiation. This reduction of net all-wave radiation of 9 Wm^{-2} produces a decrease in the daily average surface temperature of 0.4 °C, but without as much change in the amplitude in the daily cycle (Figure 5e). The energy balance has been changed with a reduction of 9 Wm^{-2} in the latent heat flux, but with no change in the sensible heat flux. All the components of evapotranspiration have been reduced: by 10 per cent for evaporation from the soil surface and the interception, and by 7 per cent for the transpiration. The different response of the direct evaporation and the transpiration is the result of a decrease of 13 per cent in the rainfall over the region (Figure 5f). The fact that latent heat flux changed in response to the reduction in net radiation whilst the sensible heat flux did not is associated with the strong reduction in rainfall. This is a positive feedback process where reduction in evapotranspiration goes on to produce a reduction in rainfall. It may be that the surface cooling which follows the increase in albedo leads to a weakening of the moisture convergence over the region and thus also contributes to the reduction in rainfall. These results are in good agreement with those of Milne and Rowntree (1992), who carried out a similar simulation with the UK Meteorological Office GCM (see their Table IVa), and with that of Dirmeyer (1992), who carried out a similar sensitivity analysis with the COLA GCM (see his Table 3.7 and 3.8).

The increase in albedo over Amazonia produces a weakening of the energy and water exchange over the region. Evapotranspiration decreases by 0.3 mm per day, rainfall by 0.7 mm per day, runoff by 0.34 mm per day, and moisture convergence by approximately 0.4 mm per day. The drier atmosphere produces a slight decrease in cloudiness at all levels in model. In practice this reduction in cloud cover produces an increase in incident solar radiation of 7 Wm^{-2} and a reduction of downward longwave radiation of 2 Wm^{-2}, this latter effect being compensated by reduction in surface temperature. These consequences of increased albedo are characteristic of the Charney effect (Charney, 1975; Charney *et al.*, 1977).

Analysing the impact of reducing the roughness length from 2 m to 0.06 m is not so straightforward as analysing the effect of increased albedo as the model responds indirectly. There is a marked increase in average windspeed at the first model level from 2.3 ms^{-1} in the control run, to 5.1 ms^{-1} for the reduced roughness experiment. Total cloudiness is reduced from an average of 67.5 to 61.2 per cent, and low cloud

Table 8 The energy and water balance of Region II of Amazonia for the period January to March inclusive of the deforestation, control, albedo change and roughness length change runs. S_D is the incident solar radiation; $(1 - \alpha)\ S_D$ is the net solar radiation; L_D is the downward longwave radiation; L_n is the net longwave radiation; R_n is the net all-wave radiation; LE is latent heat flux; H is sensible heat flux; T_s(mean), T_s(max) and T_s(min) are the mean, daily maximum and daily minimum surface temperatures; T_a is air temperature at the lowest model level; N(tot) is the percentage of total cloud cover; P is rainfall, and I is interception. Fluxes are in W m^{-2}, temperatures in °C, and rainfall and interception in mm per day.

	S_D	$(1-\alpha)$ S_D	L_D	L_n	R_n	LE	H	T_s (mean)	T_s (max)	T_s (min)	T_a	N (tot)	P	I
Control	232	203	380	65	138	112	27	24.7	32.8	19.8	25.3	68	6.2	1.12
Deforested	255	209	376	70	139	102	38	24.6	36.2	17.4	26.3	62	5.5	0.48
Albedo change	239	194	378	65	129	103	27	24.3	32.5	19.3	25.1	65	5.4	1.01
Roughness change	258	226	375	78	148	101	46	25.8	37.8	18.5	27.4	61	5.9	0.66

from 36.2 to 24.6 per cent, making a substantial change to the radiation balance (Table 8). In comparison with the control run the incident solar radiation is increased by 26 Wm^{-2} (11 per cent). There is a decrease of 5 Wm^{-2} in the downward longwave radiation, but as the surface temperature is on average 1.1°C warmer together these give an increase in longwave loss of 13 Wm^{-2}, which leads to an increase of net all-wave radiation of 10 Wm^{-2}.

The Bowen ratio changes from 0.24 in the control run to 0.46 in the roughness change experiment. This is partly a result of the less evapotranspiration, mainly caused by less interception loss, but also a result of the increased net all-wave radiation leading to a higher sensible heat flux.

The average air temperature near the surface rises by 2.1 °C in response to an increased maximum surface temperature of 5 °C. On average the decrease in roughness alone produced an increase in the daily surface temperature cycle of 6.3 °C, compared to 5.8 °C for the deforestation experiment. To strengthen the hypothesis that the increase in daily temperature amplitude found in the deforestation experiment is the result of the low roughness length of the grass, Figures 4a and 4c compare the fields of this variable for the deforestation and roughness change experiments respectively.

These sensitivity analyses are too short to produce stable rainfall fields. However, comparing Figures 4b and 4d, for the deforestation and roughness change experiments respectively, it appears that the changes to the atmospheric circulation over Amazonia after deforestation which lead to a change in rainfall are principally caused by the reduction in roughness length. This result is in agreement with that of Sud *et al.* (1988) who predicted a reduction in rainfall over Amazonia following a large reduction in roughness length, even though the energy balance had not been modified.

The results presented here are in good agreement with those of Lean and Warrilow (1989). In their simulation of the effects of reducing roughness over Amazonia they also found reduced evapotranspiration, moisture convergence and rainfall.

The sensitivity analyses presented in this section show that the effects of albedo and surface roughness play an important role in the determination of the radiation and energy balance, and in modifying the rainfall field when the forest is replaced by grass.

SENSITIVITY TO THE CONVECTION SCHEME

In introducing the ISBA scheme into the GCM EMERAUDE, Manzi and Planton (1994) emphasised the importance of considering the interactions between the surface and the other parameterizations in the model. This section looks at the interaction between the surface and convection schemes. This is achieved with two further deforestation experiments.

In the first experiment, which is the same as that described previously, the GCM is coupled to a Kuo-type cloud scheme; in the second experiment the GCM is coupled with a mass flux scheme (Bougeault, 1985). The initial conditions and the prescribed perturbations are identical for both experiments.

The results are presented as averages for the whole of Amazonia (Regions I and II), for the period January to March inclusive. The first 17 days of integration have been neglected. The model is certainly not in equilibrium at the beginning of January, however that will not affect this analysis which compares scheme response, rather than predicting the effects of deforestation.

Table 9 compares the predictions with the Kuo-type scheme. After deforestation net all-wave radiation is slightly decreased by 3 Wm^{-2}, evapotranspiration is decreased by 14 per cent, and Bowen ratio is increased from 0.16 to 0.30. The average surface temperature remains the same at 24.9 °C. The anomaly in the rainfall field (deforested minus control), presented in Figure 5a, shows a variable change in rainfall. The rainfall is reduced over the greater part of Amazonia, but it is increased in the north,

Table 9 The energy and water balance of Amazonia (Region I and II) averaged over the period January to March inclusive with EMERAUDE/ISBA coupled with a Kuo-type convection scheme. T_s(mean) is mean surface temperature (°C); E evapotranspiration; (mm per day); R_n is the net all-wave radiation (Wm^{-2}); H is sensible heat flux (Wm^{-2}); P is rainfall (mm per day); and P - E is moisture convergence (mm per day).

	T_s(mean)	E	R_n	H	P	P – E
control	24.9	4.2	142	20	7.3	3.1
deforested	24.9	3.6	139	32	6.8	3.2
deforested – control	0	-0.6	-0.3	12	-0.5	0.1

Table 10 The energy and water balance of Amazonia (Region I and II) averaged over the period January to March inclusive with EMERAUDE/ISBA coupled with a mass flux convection scheme. T_s(mean) is mean surface temperature (°C); E evapotranspiration; (mm per day); R_n is the net all-wave radiation (Wm^{-2}); H is sensible heat flux (Wm^{-2}); P is rainfall (mm per day); and P - E is moisture convergence (mm per day).

	T_s(mean)	E	R_n	H	P	P – E
control	25.6	4.0	140	22	4.7	0.7
deforested	26.6	3.6	146	41	6.7	3.1
deforested – control	1.0	-0.4	6	19	2	2.4

south and south-west.

The predictions for the mass flux scheme are compared in Table 10. In contrast to the results from the Kuo scheme, the net all-wave radiation and the average surface temperature for the grass are increased by 6 Wm^{-2} and 1 °C respectively compared to the control. The evapotranspiration is decreased by 10 per cent and the Bowen ratio changes from 0.19 to 0.39. However, it is for the moisture convergence and the rainfall that the two schemes differ most. For the mass flux scheme the rainfall for the grass increases by more than 40 per cent compared to the control, with a consequent increase of 2.4 mm per day in moisture convergence. In fact the moisture convergence over Amazonia is too weak for the forested control run, whilst it appears correct for the grassland simulation. The spatial distribution of the rainfall anomaly (deforested minus control) shows that, following deforestation, rainfall is increased over the whole of Amazonia (Figure 4b). Again showing a result in contrast to the Kuo-type scheme.

The reasons for this poor functioning of the mass flux scheme over Amazonia have not yet been established. But this analysis clearly makes the point that the predictions of climate change simulations made by GCMs must be treated with caution, because they are strongly dependent on the model formulation.

CONCLUSION

The model experiment described in this paper predicts that the impact of deforestation will be regional, with a greater impact south of the Equator. Deforestation is predicted to lead to a reduction in evapotranspiration, largely as a result of the reduced evaporation of intercepted rainfall. Rainfall is predicted to decrease in some parts of Amazonia, but increases in the north, south-west and south-east of Amazonia. In contrast to the results of other recent simulations (Lean and Warrilow, 1989; Nobre *et al.*, 1991; Dickinson and Kennedy, 1992; Polcher and Laval, 1994b) the moisture convergence and runoff are, on average, increased for the deforested case. However this effect is less apparent where the reduction in rainfall is less.

The sensitivity analyses have shown that the changes in surface roughness and albedo play an important role in determining the overall effect of deforestation, but that the type of convection scheme used in the model can also play a critical part in determining the overall conclusions that can be drawn from the simulation. The principal difference between the results reported here and those reported previously by other authors, appears to be in the model dependent schemes for the surface energy, convection, cloud, and radiative transfer. The reduction in cloud cover and the modification to the radiation balance in this simulation was also reported by Dickinson and Kennedy (1992), but not found by Lean and Warrilow (1989) or Nobre *et al.* (1991). Moisture convergence increased for this simulation, but decreased in the other studies. It can be concluded that Amazonian deforestation will change the regional climate, but more reliable estimates require improvements to made to be the GCMs' parameterisation of cloudiness and convection.

ACKNOWLEDGEMENTS

We thank Mrs Sophie Tyteca (Météo-France/CNRM) for help in conducting these simulation experiments and processing model outputs.

A.O. Manzi was partly supported by the Brazilian Conselho Nacional de Desenvolvimento Científico e Tecnológico (CNPq/RHAE). This work was also supported by the European Centre for Medium Range Weather Forecasting as part of the Special Project SPFRVESO, by the Programme National d'Etude de la Dynamique du Climat (PNEDC) and by the Commission of the European Communities (Contract EPOC-0003-C-MB).

We are grateful to John Gash for translating this paper.

REFERENCES

Bastable, H.G., Shuttleworth, W.J., Dallarosa, R.L.G., Fisch, G. and Nobre, C.A. 1993. Observations of climate, albedo and surface radiation over cleared and undisturbed Amazonian forest. *Int. J. Climatol.*, **13**, 783-796.

Bougeault, Ph. 1985. A simple parameterization of the large-scale effects of cumulus convection. *Mon. Weather. Rev.*, **113**, 2108-2121.

Brutsaert, W.H. 1982. *Evaporation into the atmosphere: theory, history and applications*. D. Reidel Publishing Company, Dordrecht.

Charney, J.G. 1975. Dynamics of deserts and drought in the Sahel. *Q. J. Roy. Meteorol. Soc.*, **101**, 193-202.

Charney, J.G., Quirks, W.J., Chow, S.H., and Kornfield, J. 1977. A comparative study of the effects of albedo change on drought in semi-arid regions. *J. Atmos. Sci.*, **34**, 1366-1385.

Coiffier, J., Ernie, Y., Geleyn, J.F., Clochard, J., Hoffman, J., and Dupont, F. 1987. The operational hemispheric model at the French Meteorological Service. *J. Meteorol. Soc. Japan, Special NWP Symposium*, 337-345.

Dickinson, R.E., and Kennedy, P. 1992. Impacts on regional climate of Amazon deforestation. *Geophysical Research Letters*, **19**, 1947-1950.

Dirmeyer, P.A. 1992. GCM studies of the influence of vegetation on the general circulation: the role of albedo in modulating climate change. *PhD thesis*, University of Maryland.

Ernie, Y. 1985. Experiments with the French spectral model. In Proceedings of 7th American Meteorological Society Conference on Numerical Weather Prediction, Montreal, 486-489.

Figueroa, S.N. and Nobre, C.A. 1990. Precipitation distribution over central and western tropical South America. *Climánalise*, **5**, 36-45.

Gash, J.H.C., Nobre, C.A., Roberts, J.M. and Victoria, R.L. 1996. An overview of ABRACOS. 1996. This volume.

Gates, W.L. 1992. AMIP: The atmospheric model intercomparison project. *Bull. Amer. Meteor. Soc.*, **73**, 36-45.

Geleyn, J.F., Bougeault, P., Rochas, M., Cariolle, D., Lafore, J.P., Royer, J.F. and André, J.C. 1988. The evolution of numerical weather prediction and atmospheric modelling at the French Weather Service. *J. Theoretical Appl. Mechanics, Suppl. 2 to vol 7*, 87-110.

Jacquemin, B. and Noilhan, J. 1990. Sensitivity study and validation of a land surface parameterization using the HAPEX-MOBILHY data set. *Bound.-Layer Meteorol.*, **52**, 93-134.

Lean, J. and Rowntree, P.R., 1993. A GCM simulation of the impact of Amazonian deforestation on climate using an improved canopy representation. *Q. J. R. Meteorol. Soc.*, **119**, 509-530.

Lean, J. and Warrilow, D. 1989. Simulation of the regional climatic impact of Amazon deforestation. *Nature*, **342**, 411-413.

Lloyd, C.R., Gash, J.H.C., Shuttleworth, W.J. and Marques, A. de O. 1988. The measurement and modelling of rainfall interception by Amazonian rain forest. *Agric. For. Meteorol.*, **43**, 277-294.

Louis, J.F., Tiedke, M. and Geleyn, J.F. 1981. A short history of the operational PBL parameterization of the ECMWF. In Workshop on Planetary Boundary Layer, ECMWF, 59-79.

Manzi, A.O. and Planton, S. 1992. Implementation of the ISBA parameterization scheme for land surface processes in a GCM. An annual cycle experiment. Notes de Centre 11, Météo-France/ CNRM/GMGEC.

Manzi, O. and Planton, S. 1994. Implementation of the ISBA scheme for land surface processes in a GCM - an annual cycle experiment. *J. Hydrol.*, **155**, 353-387.

Manzi,O. 1993. Introduction d'un schéma des transfert sol-vegetation-atmosphere dans un modèle de circulation general et application a la deforestation Amazonienne. PhD thesis, Université Paul Sabatier, Toulouse.

McWilliam, A.L.C., Roberts, J.M., Cabral, O.M.R., Leitão, M.V.B.R., de Costa, A.C.L., Maitelli, G.T. and Zamporoni, C.A.G.P. 1993. Leaf area index and above-ground biomass of *terra firme* rain forest and adjacent clearings in Amazonia. *Functional Ecol.*, **7**, 310-317.

Milne, M.F. and Rowntree, P.R. 1992. Modelling the effects of albedo change associated with tropical deforestation. *Climate Change*, **21**, 317-343.

Mintz, Y. and Serafini, Y.V. 1989. Global monthly climatology of soil moisture and water balance. *UNESCO Studies and Reports in Hydrology*.

Moore, C.J. and Fisch, G. 1986. Estimating heat storage in Amazonian tropical forest. *Agric. and Forest Meteorol.*, **38**, 147-169.

Nobre, C.A., Sellers, P.J. and Shukla, J. 1991. Amazonian deforestation and regional climate change. *J. Climate*, **4**, 957-988.

Noilhan, J. and Planton, S. 1989. A simple parameterization of land surface processes for meteorological models. *Mon. Wea. Rev.*, **117**, 536-549.

Noilhan, J., Mahfouf, J.F., Manzi, A. and Planton, S. 1992. Validation of land-surface parameterizations: Developments and experiments at the French weather service. In: *Proceedings of the workshop in validation of models over Europe*, Reading (England), ECMWF.

Planton, S., Déqué, M. and Bellevaux, C. 1991. Validation of an annual cycle simulation with a T42-L20 GCM. *Climate Dynamics*, **5**, 189-200.

Polcher, J. and Laval, K. 1994a. The impact of African and Amazonian deforestation on tropical climate. *J. Hydrol.*, **155**, 389-405.

Polcher, J. and Laval, K. 1994b. A statistical study of the regional impact of deforestation on climate

in the LMD GCM. *Climate Dynamics*, **10**, 205-219.

Rowntree, P.R. 1991. Atmospheric parameterization schemes for evaporation over land: basic concepts and climate modelling aspects. In: *Land Surface Evaporation - Measurement and Parameterization*, (Eds. T.J. Schmugge and J.C. André). Springer-Verlag. 5-29.

Royer, J.F., Planton, S. and Déqué, M. 1990. A sensitivity experiment for the removal of Arctic Sea ice with the French Spectral General Circulation Model. *Climate Dynamics*, **5**, 1-17.

Shuttleworth, W.J. 1988. Evaporation from Amazonian rain forest. *Proc. Roy. Soc.(Lond.) B*, **233**: 321-346.

Shuttleworth, W.J., Gash, J.H.C., Lloyd, C.R., Moore, C.J., Roberts, J., Marques, A. de O., Fisch, G., Silva, V. de P., Ribeiro, M.N.G., Molion, L.C.B., de Abreu Sa, L.D., Nobre, C.A., Cabral, O.M.R., Patel, S.R. and de Moraes, J.C. 1984a. Eddy correlation measurements of energy partition for Amazonian forest. *Q.J. Roy. Meteorol. Soc.*, **110**, 1143-1162.

Shuttleworth, W.J., Gash, J.H.C., Lloyd, C.R., Moore, C.J., Roberts, J., Marques, A. de O., Fisch, G., Silva, V. de P., Ribeiro, M.N.G., Molion, L.C.B., de Abreu Sa, L.D., Nobre, C.A., Cabral, O.M.R., Patel, S.R. and de Moraes, J.C. 1984b. Observations of radiation exchange above and below Amazonian forest. *Q.J. Roy. Meteorol. Soc.*, **110**, 1163-1169.

Sud, Y.C., Shukla, J. and Mintz, Y. 1988. Influence of land surface roughness on atmospheric circulation and rainfall: a sensitivity study with a General Circulation Model. *J. Appl. Meteor.*, **27**, 1036-1054.

Wilson, M.F. and Henderson-Sellers, A. 1985. A global archive of land cover and soils data sets for use in General Circulation Climate Models. *J. Climatol.*, **5**, 119-143.

Wright, I.R., Gash, J.H.C., da Rocha, H.R., Shuttleworth, W.J., Nobre, C.A., Maitelli, G.T.M., Zamparoni, C.A.G.P. and Carvalho, P.R.A. 1992. Dry season micrometeorology of central Amazonian ranchland. *Q.J. Roy. Meteorol. Soc.*, **118**, 1083-1099.

RESUMO

As parametrizações dos processos de superfície usadas nos MCGA (Modelos de Circulação Geral da Atmosfera) foram bastante aprimoradas na última década, com a inclusão de uma representação explícita da vegetação e dos processos físicos relacionados a ela. No CNRM (Météo-France) um novo esquema, chamado de esquema ISBA (Interações entre Solo, Biosfera e Atmosfera) desenvolvido por Noilhan e Planton (1989), foi implementado no AGCM Espectral EMERAUDE (Manzi e Planton, 1994). Este acoplamento ISBA/AGCM é uma ferramenta poderosa para se investigar mudanças de origem natural e antropogênica nas superfícies continentais, como os processos de desertificação ou desmatamento. Neste artigo são apresentados resultados de uma simulação de desmatamento de 4 anos sobre a Amazônia, onde a floresta tropical chuvosa natural e as savanas de uma extensa área da América do Sul foram substituídas por pastagens degradadas. O esquema ISBA foi testado cuidadosamente usando dados dos experimentos observacionais ARME (Experimento Micrometeorológico da Região Amazônica) e ABRACOS, respectivamente, para floresta e pastagem. A simulação com a Amazônia desmatada mostrou um enfraquecimento do ciclo hidrológico e uma amplificação do ciclo diurno da temperatura de superfície quando comparada com a simulação de controle. Um estudo de sensitividade mostrou a grande importância do albedo de superfície e do comportamento da rugosidade na resposta ao desmatamento.